Tellus (2005), 57B, 332–340
Printed in Singapore. All rights reserved

TELLUS

Tracer-derived transit time of the waters in the eastern Nordic Seas

By YONGQI GAO[1,2,3]*, HELGE DRANGE[1,2,3,4], MATS BENTSEN[1,2] and OLA M. JOHANNESSEN[1,4,5], [1]*Nansen Environmental and Remote Sensing Center, Bergen, Norway;* [2]*Bjerknes Centre for Climate Research, Bergen, Norway;* [3]*Nansen-Zhu International Research Centre, Beijing, China;* [4]*Geophysical Institute, University of Bergen, Norway;* [5]*Mohn-Sverdrup Center for Global Ocean Studies and Operational Oceanography, Bergen, Norway*

(Manuscript received 13 July 2004; in final form 8 March 2005)

ABSTRACT

The spatial-temporal distribution of the anthropogenic radionuclide ^{137}Cs originating from nuclear bomb testing and the Sellafield reprocessing plant in the Irish Sea is simulated using a global version of the Miami Isopycnic Coordinate Ocean Model (MICOM). The physical model has a horizontal resolution of about 40 km, and it is forced with daily atmospheric reanalysed fields for the period 1948 to 2002. A comparison of the temporal evolution of observed and simulated concentrations of ^{137}Cs has been conducted for the regions east of Scotland, west of central Norway and at the entrance of the Barents Sea. It follows that the annual mean ^{137}Cs concentration signal from the Sellafield discharge reaches the southwestern Barents Sea region in 5 yr, in accordance with available observations. To more accurately assess the age of the caesium-tagged water masses, three additional experiments were performed with an Eulerian age coupled to the evolution of the tracer concentration. It is demonstrated that the transit time depends on the duration of the tracer release history, on the dynamical ocean state and on whether the transit time is derived from the time difference between the release history and the concentration evolution downstream of the release, or as an explicit Eulerian age tracer. The Eulerian age tracer gives a transit time for a Sellafield-like discharge to reach the Barents Sea of 56 months in the 1970s, 52 months in the 1960s and 51 months in the 1980s, and that this difference is strongly governed by the ocean dynamics in the Faeroe–Scotland region.

1. Introduction

Tracers with known temporal and spatial source functions are well suited to shed light onto processes and mechanisms that are not easily deduced from the basic, observed or simulated, ocean state variables. For instance, radionuclides from the atmospheric nuclear bomb tests in in the 1950s and 1960s and chlorofluorocarbons (CFCs) emitted to the atmosphere since the 1930s have been used to explore the regional to global decadal-scale ventilation of the ocean surface waters (England and Maier-Reimer, 2001; Aoyama and Hirose, 2003; Willey et al., 2004), whereas natural radiocarbon has been used to map the path and age of the global overturning circulation (Toggweiler et al., 1989a,b). Other radionuclides like caesium-137 (^{137}Cs), strontium-90 (^{90}Sr) and technetium-99 (^{99}Tc) originating from nuclear fuel reprocessing plants have been used to explore the local and basin-scale transport and dispersion of the waters exposed to these discharges (Dahlgaard, 1995; Brown et al., 2002; Gao et al., 2004; Karcher et al., 2004).

In this study ^{137}Cs from the UK's Sellafield reprocessing plant in the Irish Sea is used to illuminate the transport and dispersion of waters from this location, and then in particular the exposed northward-flowing Atlantic and Norwegian coastal waters in the eastern part of the Nordic Seas. The objectives of the study are:

(1) To evaluate the simulated transport of ^{137}Cs from Sellafield in a global, intermediate-resolution climate-type ocean general circulation model (OGCM).

(2) To deduce the concentration and the Eulerian-derived age of the Sellafield-tagged waters in the Nordic seas region.

(3) To explore differences between continuous (multi-annual) and pulse (single-year) ^{137}Cs-like releases from the Sellafield location in the Irish Sea.

(4) To address possible variations in the tracer-derived age of the waters in the eastern Nordic Seas over the last 50 yr.

The paper is organized as follows. A description of the model system and the experimental design is given in Section 2,

*Corresponding author.
e-mail: yongqi.gao@nersc.no

and the obtained results are presented in Section 3. The paper is then continued by discussions (Section 4) and conclusions (Section 5).

2. Model description and experimental design

2.1. OGCM

The OGCM applied in this study is the Miami Isopycnic Coordinate Ocean Model (MICOM) (Bleck et al., 1992), fully coupled to a sea-ice module consisting of the Hibler (1979) rheology in the implementation of Harder (1996), and the thermodynamics of Drange and Simonsen (1996). The model system is a modification of the system used by Gao et al. (2004) (hereafter G04) to study the transport of non-Chernobyl ^{137}Cs and ^{90}Sr in the North Atlantic–Arctic region. The main modifications to G04 are doubled horizontal resolution and reduced strength of the parameterized isopycnal and diapycnal mixing rates, the latter based on the CFC model evaluation study by Gao et al. (2003).

Specifically, the horizontal grid resolution is about 40 km in the northern North Atlantic/Nordic Seas region, and the diffusive velocities (diffusivities divided by the size of the grid cell) for layer interface diffusion, momentum dissipation and tracer dispersion are 0.015, 0.01 and 0.0025 m s^{-1}, respectively. The diapycnal mixing coefficient K_{d} (m^2 s^{-1}) is parameterized as $K_{\mathrm{d}} = (5 \times 10^{-8})/N$, where N (s^{-1}) is the Brunt–Väisälä frequency. Consequently, the values of tracer dispersion and diapycnal mixing are a factor 2 and 6, respectively, below those used in G04.

The model is initialized and spun-up following the procedure in G04. The applied forcing is also identical to G04, i.e. daily atmospheric reanalysis fields for the period 1948–2002 provided by NCAR/NCEP (Kalnay et al., 1996).

The results presented here are based on integration cycle number 2 with NCAR/NCEP forcing (i.e. the integration after the first spin-up of 55 yr with daily NCAR/NCEP forcing, starting cycle 2 with the full model state at the end of cycle 1). The tracer experiments have also been conducted in a third cycle with NCAR/NCEP forcing. The obtained results from cycles 2 and 3 are very similar, indicating robustness of the obtained results to the applied spin-up procedure and the essentially unknown 1948 initial ocean state. For clarity, only the results from cycle number 2 are presented here.

2.2. Tracer module

Three types of tracers have been used in the study, the soluble and assumed dynamically passive radionuclide ^{137}Cs with a half-life of 30.1 yr, an idealized and conservative tracer C* without decay, and an age tracer representing the Eulerian age of water masses tagged with C*.

Although ^{137}Cs is often considered to be conservative, as in this study, sediments in suspension and at the sea bed could play a role in the Irish Sea (Woodhead and Pentreath, 1992). There is evidence that ^{137}Cs stored in the sediments is now desorbing to the water column. However, there is no published evidence that desorption of the Sellafield-supplied ^{137}Cs occurs outside the Irish Sea (Kershaw and Baxter, 1995). The remobilization of ^{137}Cs from the Irish Sea sediments currently contributes about 1 Bq m^{-3} of the contribution from Sellafield to the Norwegian Coast Current (Poole et al., 1997). The assumption of ^{137}Cs as a conservative tracer is thus, to lowest order, justified.

The spatial-temporal evolution of the Eulerian concentration C and age A (s) of a conservative and non-decaying tracer are governed by the conservation equations (England, 1995; Delhez et al., 1999; Delhez and Deleersnijder, 2002)

$$\frac{\partial C}{\partial t} + \nabla \cdot (\mathbf{u}C) = \nabla \cdot (K \nabla(\mathbf{u}C)) + F_{\mathrm{C}} \tag{1}$$

$$\frac{\partial AC}{\partial t} + \nabla \cdot (\mathbf{u}AC) = \nabla \cdot (K \nabla(\mathbf{u}AC)) + C. \tag{2}$$

Here t (s) is time, $\mathbf{u}$ (m s^{-1}) is the velocity, K (m^2 s^{-1}) is the diffusion coefficient, ∇ (m^{-1}) is the grad operator and F_{C} is the source rate of tracer C. For a radioactive tracer C, like ^{137}Cs, the concentration is commonly expressed in terms of Bq m^{-3}, and the above equations are modified by appropriate decay terms on the right-hand side of the equations (see below).

The age A of the tracer can be viewed as an inherent property, or an attribute, of the tracer. The age is set to zero for the source waters, and increases linearly with time since the release. For any model grid cell, the Eulerian concentration C from (1) represents the sum of subtracers that have been released at different times and have followed different pathways. With incorporation of the age tracer, each of these subtracers has their own age. The age A derived from (2) is therefore the concentration-weighted mean age of each subtracer in any model grid cell, or what we will name the apparent age hereafter.

2.3. The Sellafield discharge

The major sources for the radionuclide ^{137}Cs in the North Atlantic–Arctic region are the nuclear bomb testing in the 1950s and 1960s, the 1986 Chernobyl accident and the discharges from the European reprocessing plants at Sellafield on the Irish Sea and Cap de La Hague on the French coast of the English Channel (Nies et al., 1998). The Sellafield discharge has been dominant over that of Cap de La Hague in terms of quantities and impact for the majority of the northern waters (Kershaw and Baxter, 1995). Therefore, only the dispersion of ^{137}Cs released from the Sellafield plant (see Fig. 1) has been considered in this study. The annual mean time evolution of ^{137}Cs from Sellafield and the nuclear bomb testing are fairly well known and have been provided by S. Nielsen (personal communication, 2001; see also Fig. 3 in G04). The present study does not include input from the Chernobyl accident.

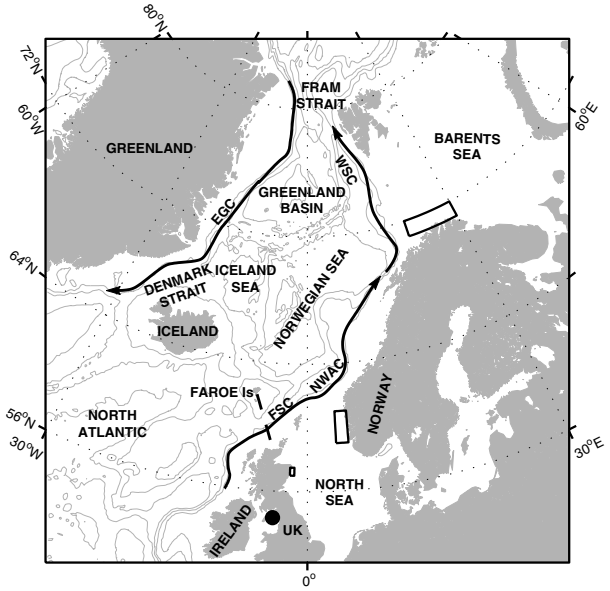

Fig. 1. Schematic of the region of interest. The location of the Sellafield plant is indicated with the black dot in the Irish Sea. The Faeroe–Shetland transect is shown with the dashed line, and the locations of the observations are shown as rectangles east of Scotland (57.0–57.5°N, 1.5–2.0°W), west of Norway (59–61°N, 3.5–5.0°E) and in the southwestern Barents Sea region (71–72°N, 20–30°E). FSC is the Faeroe–Scotland Channel, NWAC is the Norwegian Atlantic Current, WSC is the West Spitsbergen Current and EGC is the East Greenland Current.

The Sellafield discharge of ^{137}Cs is included in the OGCM by releasing it into the mixed layer (ML) grid cell closest to the actual Sellafield release location. The tracer simulation starts with zero concentration of ^{137}Cs in 1950.

2.4. Experimental design

A set of four experiments were performed. In experiment 1 (E1), the spreading and mixing of the Sellafield ^{137}Cs discharge and the atmospheric fallout were simulated for the period 1950 to 2002. This integration attempts to provide a realistic realization of the time–space distribution of ^{137}Cs, and is the simulation against which the observed concentration of ^{137}Cs has been evaluated. Experiment 1 is the only model run that includes radioactive decay of ^{137}Cs. This is implemented by the term $-C/\tau$ on the right-hand side of eq. (1), where $\tau = 30.1$ yr is the half-life of ^{137}Cs.

The remaining simulations are idealized in that the Sellafield-like tracer C* has no radioactive decay, that only the Sellafield release rates of ^{137}Cs for the 7 yr period 1975–1981 are taken into account, and that the global concentration of C* at 1 January 1975 is set to zero. In addition to the 7 yr Sellafield release of C*, a single-year release of C* representing the year 1975 is included. In this way, a continuous (7 yr) and a pulse (1 yr) release of C* are compared, both starting at 1 January 1975. Furthermore, the age tracer *A* is coupled to the 7 yr continuous release of C*, yielding an apparent age estimation of the water masses exposed to the continuous release of C*.

Experiment 2 (E2) uses the atmospheric forcing from the period 1975–1984 and starts from the physical restart file of E1 from 1 January 1975. Experiment 3 (E3) is identical to E2 but uses the atmospheric forcing for the period 1958–1965 and the physical restart file from E1 from 1 January 1958. Likewise, experiment 4 (E4) is identical to E2 but uses the atmospheric forcing for the period 1980–1987 and the physical restart file from E1 from 1 January 1980. Experiments 2–4 therefore provide a measure of the temporal variability of a Sellafield-like ^{137}Cs tracer release for the time periods 1975–1984, 1958–1965 and 1980–1987, respectively. The reasons for using for the time periods of E3 and E4 are given below.

3. Results

A description of the simulated circulation and hydrography in the region of interest, e.g. for the northern North Atlantic and the Nordic Seas, will not be given here as these quantities have been addressed in the studies of Furevik et al. (2002), Gao et al. (2003, 2004), Nilsen et al. (2003), Hatun et al. (2005) and Eldevik et al. (2005) for model systems closely related to the one used here. In general, the model system has demonstrated skill in simulating the ocean circulation and thermodynamics in the region of interest.

A quantity of expected importance for a successful simulation of the Sellafield release is the intensity of the northward flow of Atlantic water between the Faeroes and Scotland, hereafter the Faeroe–Scotland Channel (FSC) (see Fig. 1). The simulated northward transport through the FSC is given in Fig. 2a, with a mean value for the period 1948–2002 of 3.6×10^6 m^3 s^{-1}. A recent current meter-derived estimate of the Atlantic inflow to the Nordic Seas in the FSC for the period October 1998 to December 2001 is 4.0×10^6 m^3 s^{-1} (Østerhus et al., 2005). The corresponding number given by the applied model system is 3.8×10^6 m^3 s^{-1}. Furthermore, an evaluation of the temporal variability of the simulated northward volume transport through the FSC has been conducted by comparing the monthly normalized anomalies of the simulated and observed transports between October 1998 and December 2001 (Fig. 2b). The favourable comparison of the mean transport (4.0×10^6 versus 3.8×10^6 m^3 s^{-1}) and the temporal variability of the flow (Fig. 2b) adds credit to the model system.

Unfortunately, no direct and continuous current meter-derived estimates of the inflow are available prior to October 1998. However, fairly realistic simulated transports across the Greenland–Scotland ridge for the 1990s (Nilsen et al., 2003), and a representative description of the temperature of the northward-flowing Atlantic water on the Scottish slope (Hatun et al., 2005) for the period 1948 to present indicate that the model system is able to

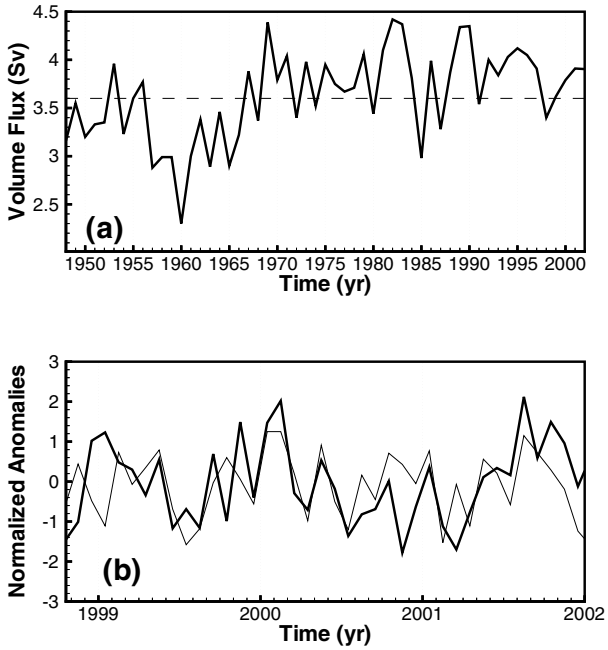

Fig. 2. (a) Simulated time-series of the annual northward volume transport [in Sv (1 Sv = 10^6 m^3 s^{-1})] through the Faeroe–Scotland Channel (FSC, see Fig. 1) with the dashed line denoting the mean value between 1948 and 2002 of 3.6 Sv. (b) The normalized anomalies of the observed (Østerhus et al., 2005) (thin line) and the simulated northward volume transports for the time period October 1998 to December 2001 (thick line).

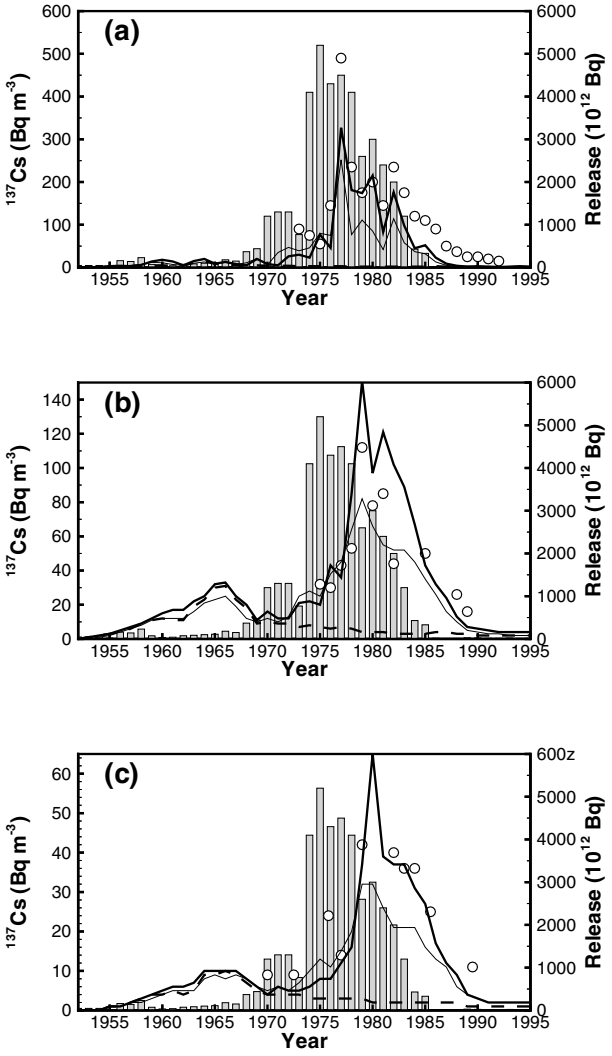

Fig. 3. Time-series of the Sellafield release rates of ^{137}Cs (10^{12} Bq yr^{-1}; bars), the observed ^{137}Cs surface concentration (Bq m^{-3}) from Kershaw and Baxter (1995) in circles, the simulated surface concentration due to the atmospheric fallout (dashed line) and the sum of the concentrations from the Sellafield release and the atmospheric fallout (thick solid line) for the east of Scotland (a), west of Norway (b) and in the southwestern Barents Sea region (c). For comparison, the thin line corresponds to the thick solid line, but is taken from the 80 km resolution version of the model (Gao et al., 2004). Note the different concentration scales on the panels. The locations are given in Fig. 1.

reproduce important quantities of the Atlantic inflow in the FSC region.

From the simulated time-series in Fig. 2a, clear interannual to decadal variations in the northward transport through the FSC are seen. For instance, low transport values are found around 1960 and relatively high transports are obtained in the early 1980s. The time periods for E3 (1958–1965) and E4 (1980–1987) are based on these rather anomalous inflow situations.

To qualitatively and quantitatively evaluate the simulated transport and mixing of the Sellafield discharge, time-series of observed and simulated surface ^{137}Cs concentration east of Scotland, west of Norway and in the southwestern Barents Sea region (see Fig. 1) are provided in Fig. 3. Clearly, the atmospheric fallout dominates the surface ^{137}Cs distributions in the mid-1960s in the three regions. However, from the late 1970s to the late 1980s, the Sellafield discharge heavily dominates the evolution of the surface ^{137}Cs concentration. For the last 5–10 yr of the simulation, the surface concentrations of ^{137}Cs are again mainly governed by atmospheric fallout. The temporal and spatial evolution of the surface ^{137}Cs concentrations are in broad agreement with observations (Fig. 3), and are, in general, superior to the results in G04 (thin solid line in Fig. 3).

To assess the influence of the duration of the release history on the transit time derived from the peak concentrations, Fig. 4 shows annual mean time-series of the surface C* concentration induced by the pulse (1 yr) and the continuous (7 yr) C* releases at the entrance of the Barents Sea in E2, E3 and E4. For comparison, time-series of the monthly mean surface C* concentration and apparent age from the continuous (7 yr) release experiments are displayed in Fig. 5. Finally, the spatial distribution of the apparent age distribution of C* averaged over the last year of E2 is provided in Fig. 6a. In panels (b) and (c) of

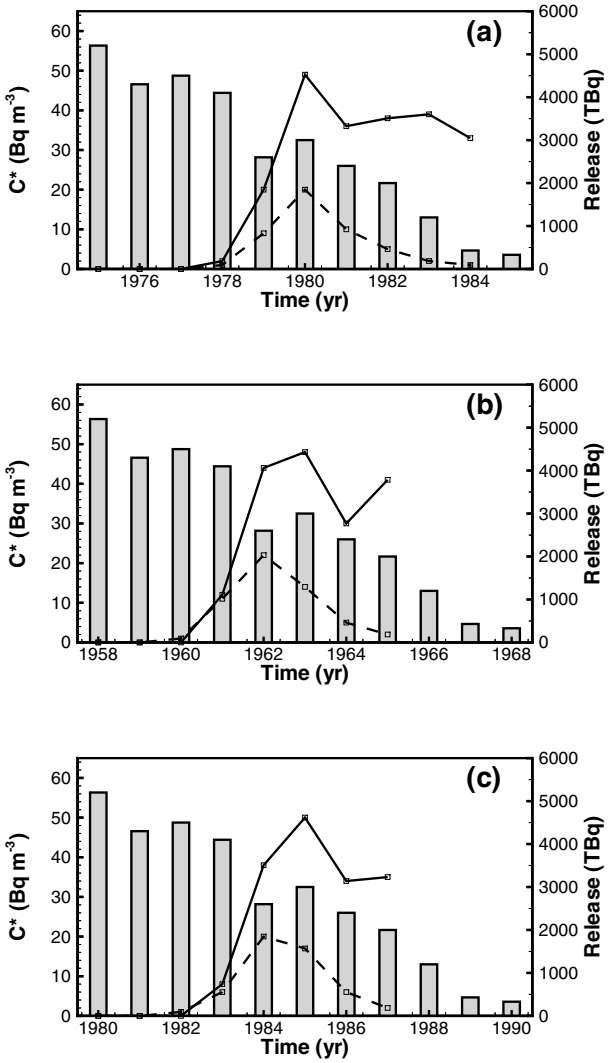

Fig. 4. Simulated time-series of the Sellafield release rates of C* (10^{12} Bq yr^{-1}; bars), and the surface concentrations (Bq m^{-3}) for the pulse/continuous release (dashed/solid line) in the southwestern Barents Sea. The experiments started at 1 January 1975 (a), 1958 (b) and 1980 (c), respectively. The relative time denotes the time since the start of the experiments.

Fig. 6, the difference in the apparent age between E2 and E3/E4 is provided.

4. Discussion

4.1. Pathway of ^{137}Cs

The applied model system is able to reproduce several of the characteristic features of the observed ^{137}Cs field downstream of the release site (Fig. 3). The most noticeable differences are too low concentrations off Scotland, particularly in 1977 and in the mid-1980s, and too high concentrations off the coast of

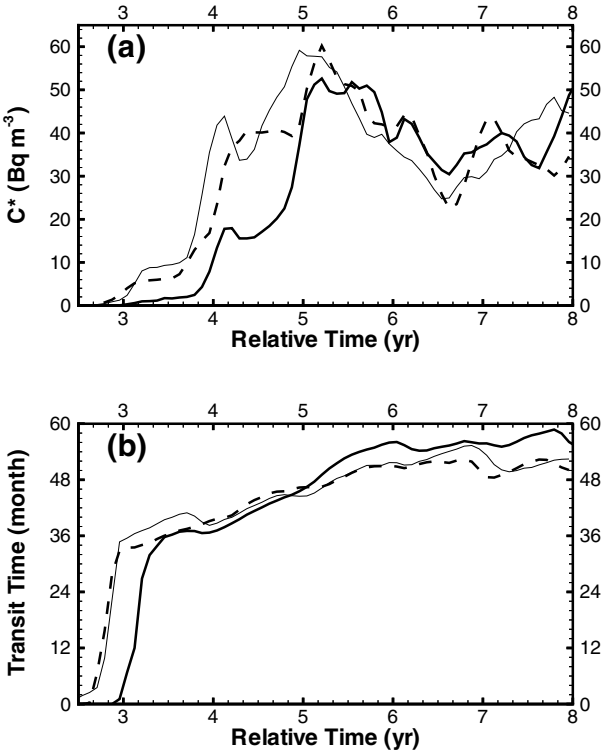

Fig. 5. (a) Simulated time-series of the surface monthly mean C* concentration (Bq m^{-3}) at the southwestern Barents Sea and (b) the corresponding apparent age (in months) for the continuous release case. The thick, thin and dashed lines represent E2, E3 and E4, respectively. The apparent age averaged over years 6 to 8 are 56, 52 and 51 months, respectively (from panel b).

Norway in the early 1980s. It is possible that these differences, and then particularly the differences off Scotland, are caused by unresolved and thus inappropriate coastal dynamics in the applied 40 km model system. For the Barents Sea, the 1976 observation is apparently inconsistent with the Sellafield release history, whereas the relatively high concentration value in 1989 is possibly caused by the non-simulated Chernobyl accident in 1986.

The simulated pathway (Fig. 6a) of C* is broadly consistent with the known transport routes of the Atlantic water in the Nordic Seas: Initially the tracer is carried northwards from the Irish Sea as a plume-like structure via the North Channel. It then partly flows along the northern coast of Scotland into the North Sea (Kershaw and Baxter, 1995), and partly follows the shelf break northward off the coast of Norway (Orvik and Skagseth, 2003). Off northern Norway, one branch extends eastwards into the Barents Sea and the other towards the Fram Strait, becoming the West Spitsbergen Current (WSC). Near the Fram Strait, part of the Atlantic water recirculates and continues southwards, joining the East Greenland Current (EGC), whereas the remaining part subducts and enters the Arctic Ocean under the upper, low-salinity Arctic surface water.

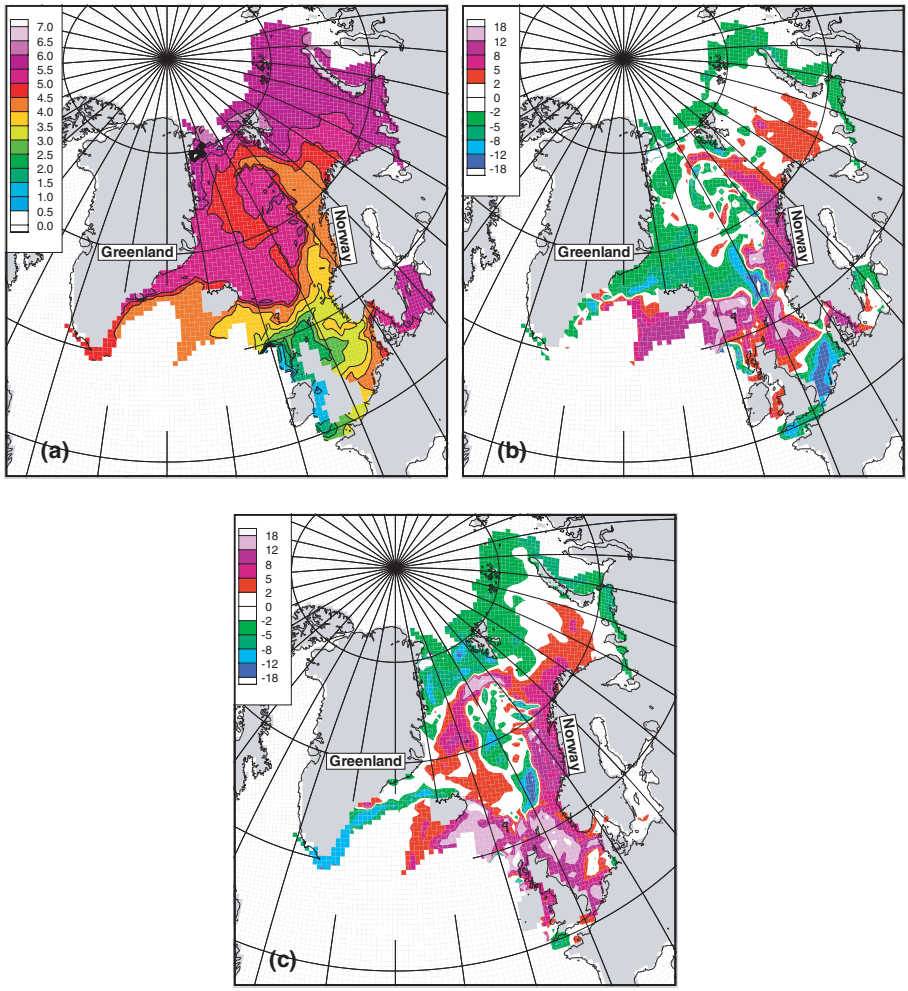

Fig. 6. (a) The mean apparent age (yr) distribution in 1981 of the Sellafield release of C* in E2. Parts (b) and (c) show the apparent age difference of surface water in months between E2 and E3, and between E2 and E4, respectively.

4.2. Transit time

The observation-based transit time of a tracer is commonly defined as the time between peak release rates and the corresponding downstream concentration peak of the tracer. In E1, the transit time at eastern Scotland is about 2 yr, about 4 yr for western Norway and about 5 yr for the southwestern Barents Sea (Fig. 3). The obtained transit times are in accordance with earlier observation-based studies (Kershaw and Baxter, 1995; Livingston et al., 1984), as well as model studies (Nies et al., 1998; Gao et al., 2004; Karcher et al., 2004). Furthermore, Brown et al. (2002) found that the transit time is 3.5 yr (42 months) for the Sellafield signal to reach the northern coast of Norway based on cross-correlation analysis of observed ^{99}Tc in the 1990s. For comparison, the idealized C* tracers used in this study give transit times at the northern coast of Norway of 4.2 yr for E2, and 3.7 yr for E3 and E4, and thus give transit times close to that of ^{99}Tc in the 1990s.

The time history of the tracer release rate will, in general, influence the transit time when the latter is based on comparison between peak release and peak concentration time histories. This is illustrated in Fig. 4 showing the concentration evolution of C* in the Barents Sea for pulse (1 yr) and continuous (7 yr) release histories. The transit time is also time-variant as a result of variations in the dynamical state of the system (see below).

4.3. Apparent age distribution

To obtain more accurate estimates of the transit time for a given release history and for a specific time period, the evolution of monthly mean concentration histories (Fig. 5a), or better, the apparent age (Fig. 5b) of a given tracer, should be considered. Whereas the first quantity can be deduced from observations, the latter can only be obtained from a model. It follows from Fig. 5b that the mean apparent age for the continuous tracer in

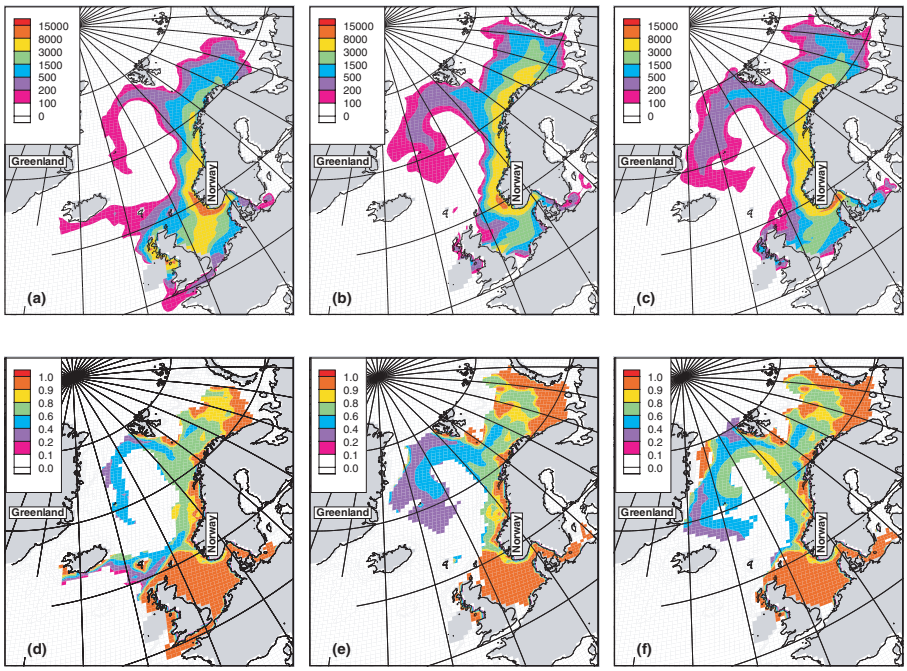

Fig. 7. Simulated vertically integrated inventories of C* (Bq m^{-2}) in the upper 200 m averaged over year 4 of the pulse release experiments (a–c) and the ratio of the upper 200 m inventory to the total inventory (d–f). Left, middle and right columns display experiments E2, E3 and E4, respectively.

experiments E2–E4 at the Barents Sea are 56, 52 and 51 months, respectively.

Depending on the problem at hand, the 5 month difference between E2 and E4 may or may not be of significance. However, from the spatial apparent age distribution in Figs 6b and 6c, it follows that regions in the North Sea and the Nordic Seas may experience differences in the apparent age of an idealized Sellafield-like tracer by up to 2 yr.

It is interesting to note that the apparent age of E3 and E4 have several features in common despite the difference in the strength of the poleward flow in the FSC (see Fig. 2) between the two experiments. This illustrates that the poleward transport in the FSC is a far too simple index to use to explain variations in the simulated apparent age. A combination of transport and mixing processes governs the evolution of Sellafield tracers in the Nordic Seas. This is illustrated in Fig. 7, showing the vertically integrated inventories of C* in year 4 of the pulse release experiments over the upper 200 m of the water column, and the ratio of the upper 200 m inventory to the total inventory. From the surface distribution of the tracer (upper panels in Fig. 7), it follows that a relatively large portion of the tracer is present in the FSC and the English Channel in E2, whereas E3 and E4 are relatively similar with more of the tracer going into the Barents Sea and recirculating in the western part of the Nordic Seas.

The integrated effect of vertical mixing follows from the lower panels in Fig. 7. In the region around the Faeroe Islands, the tracer has been strongly entrained into the subsurface waters in E2, but not in E3 and E4. This is not caused by differences in the thickness of the simulated upper ML, as the weekly evolution of the ML thickness is very similar between the three experiments in the FSC region (not shown), but by an interplay between the annual ML cycle and the transport of the tracer into and out of the FSC region. Specifically, the differences in the local wind forcing between the three experiments lead to westward transport of C* in E2 during years 2 and 3 of the experiment, no westward transport at all in E4, and a weak westward transport only during year 3 in E3. The net effect of these transport differences in year 4 follows from the lower panels of Fig. 7.

It follows from Fig. 8 that the E2 tracer enters the FSC region later than in E3 and E4. The E2 tracer experiences deep mixing three times (winters in years 2, 3 and 4), whereas the E3 and E4 tracers are being advected northwards and out of the FSC region after year 3. The E2 tracer is in this way partially trapped in the FSC region, and a fraction of the tracer even extends westwards on the southern flank of the Iceland–Faeroe ridge (Figs 7a and d). The trapping of the tracer in the FSC region leads to a lower concentration at higher latitudes in E2 compared with E3 and E4. Other features of experiments E2 to E4 are

(1) The monthly mean evolution of the tracer signal in E2–E4 at the Barents Sea entrance (Fig. 5) strongly indicate that continuous (monthly resolved) observations are required to uniquely determine the passage of a peak concentration signal downstream of a Sellafield-like source

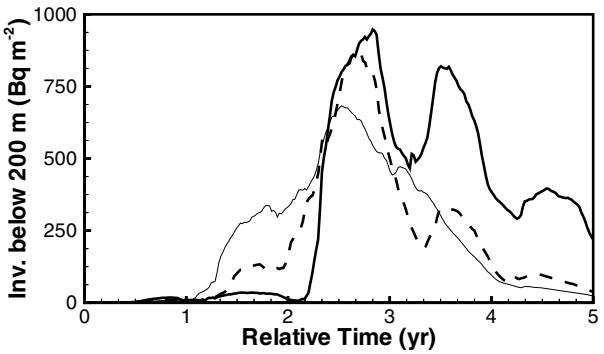

Fig. 8. Simulated time-series of the weekly mean C* inventory (Bq m^{-2}) in the FSC region (57°N to 62°N, 10°W to the Greenwich meridian) below 200 m of the pulse experiments. The thick, thin and dashed lines represent E2, E3 and E4, respectively.

(2) The E3 tracer is up to 1 yr older than the E2 tracer in the southeastern North Sea. This difference is caused by weaker flow of Atlantic water into the North Sea north of Scotland in the early 1960s compared with the late 1970s/early 1980s. This also follows from Figs 7b and c

(3) Both E3 and E4 yield water masses about 8 months younger in the Lofoten Basin (located off the coast of Norway at about 66°N) compared with E2. The reason for this is the deep mixing along the Iceland–Scotland ridge in E2, trapping Sellafield-exposed water masses there.

5. Conclusions

In this study, the ocean component of the Bergen climate model (Furevik et al., 2003; Bentsen et al., 2004), forced with daily atmospheric reanalysis fields, has been used to address the transport of ^{137}Cs from the Sellafield nuclear reprocessing plant in the Irish Sea. Special attention has been paid to the poleward transport of waters in the eastern part of the Nordic Seas. The horizontal resolution of the applied model system is 40 km over the northern North Atlantic and the Nordic Seas region, or close to the current generation of coupled atmosphere–sea ice–ocean climate models. The obtained results are therefore transferable to, and provide an excellent test-bed for, many of the model systems currently used for the Fourth Assessment Report of the Intergovernmental Panel of Climate Change (IPCC) scheduled for 2007.

Four experiments have been conducted. The first experiment (E1) provides a realistic simulation of ^{137}Cs released from the Sellafield reprocessing plant in the Irish Sea for the time period 1950–2002. The other experiments show model realizations of the transport of idealized ^{137}Cs tracers for the period 1975–1984 (E2), 1958–1965 (E3) and 1980–1987 (E4). Both the spatial distribution of the apparent age tracer (Fig. 6a) and the differences between the apparent age tracers between the three experiments (Figs 6b and c) illustrate the power of combining observations and models in assessing the temporal and spatial distribution of transit time.

In summary, the observation–model evaluation and model simulations presented here have demonstrated the following:

(1) Accurate transit times derived from observations require continuous (i.e. monthly) monitoring of the concentration downstream of a tracer source (Fig. 5a).

(2) Transit times based on peak concentrations depends on the duration of the source signal (pulse versus continuous release) and on the dynamical state of the system (Fig. 4)

(3) Model systems can be used as a quick and cost-effective laboratory for diagnosing transport and mixing processes of observed tracers (Fig. 7)

(4) The Sellafield ^{137}Cs tracer is an excellent tracer for regional and global model evaluation, even for climate-type OGCMs (Figs 3 and 8)

(5) The current generation of OGCMs is suitable for useful one-to-one comparisons between observed and simulated point-source tracer fields.

6. Acknowledgments

The authors would like to thank Dr Sven Nielsen at the Risø Laboratory, Denmark for providing time histories of the ^{137}Cs Sellafield release rates, Dr Bill Turrell at the Fisheries Research Service, Scotland for providing the Faroe–Scotland–Channel flow estimate and Dr Jan Even Øie Nilsen at the Nansen Center for generating Fig. 1. The study is a part of the project *Arctic Radioactive Contamination* (ARC), funded by the Research Council of Norway (RCN). The model development has received support from RCN through, in particular, *RegClim* and the *Programme of Supercomputing*. Support from the G. C. Rieber Foundations is acknowledged. This is contribution no A92 from the Bjerknes Centre for Climate Research.

References

Aoyama, M. and Hirose, K. 2003. Temporal variation of ^{137}Cs water column inventory in the North Pacific since the 1960s. *J. Environ. Radioactivity* **69**, 107–117.

Bentsen, M., Drange, H., Furevik, T. and Zhou, T. 2004. Simulated variability of the Atlantic meridional overturning circulation. *Clim. Dyn.* **22**, 701–720, doi:10.1007/s00382-004-0397-x.

Bentsen, M., Evensen, G., Drange, H. and Jenkins, A. D. 1999. Coordinate transformation on a sphere using conformal mapping. *Mon. Weather Rev.* **127**, 2733–2740.

Bleck, R., Rooth, C., Hu, D. and Smith, L. T. 1992. Salinity-driven thermohaline transients in a wind- and thermohaline-forced isopycnic coordinate model of the North Atlantic. *J. Phys. Oceanogr.* **22**, 1486–1515.

Brown, J., Iospje, M., Kolstad, K., Lind, B., Rudjord, A. and co-author 2002. Temporal trends for ^{99}Tc in Norwegian coastal environments and spatial distribution in the Barents Sea. *J. Environ. Radioactivity* **60**, 49–60.

Dahlgaard, H. 1995. Transfer of European coastal pollution to the Arctic: radioactive tracers. *Mar Pollut Bull.* **31**, 3–7.

Delhez, E., Campin, J. and Deleersnijder, E. 1999. Toward a general theory of the age in ocean modelling. *Ocean Model.* **1**, 17–27.

Delhez, E. J. and Deleersnijder, E. 2002. The concept of age in marine modelling II. Concentration distribution function in the English Channel and the North Sea. *J. Mar. Syst.* **31**, 279–297.

Drange, H. and Simonsen, K. 1996. *Formulation of Air–Sea Fluxes in the ESOP2 Version of MICOM*. Technical Report 125, Nansen Environmental and Remote Sensing Center, Solheimsviken, Norway.

Eldevik, T., Straneo, F., Sando, A. and Furevik, T. 2005. Pathways and export of Greenland Sea Water. In: *The Nordic Seas*, American Geophysical Union Geophysical Monograph. American Geophysical Union, Washington, DC, pp. 89–104.

England, M. 1995. The age of water and ventilation timescales in a global ocean model. *J. Phys. Oceanogr.* **25**, 2756–2777.

England, M. and Maier-Reimer, E. 2001. Using chemical tracers to assess ocean models. *Rev. Geophys.* **39**, 29–70.

Furevik, T., Bentsen, M., Drange, H., Johannessen, J. A. and Korablev, A. 2002. Temporal and spatial variability of the sea surface salinity in the Nordic Seas. *J. Geophys. Res.* **107**, 8009, doi:10.1029/2001JC001118.

Furevik, T., Bentsen, M., Drange, H., Kindem, I., Kvamstø, N. and co-author 2003. Description and validation of the Bergen Climate Model: ARPEGE coupled with MICOM. *Clim. Dyn.* **21**, 27–51, doi:10.1007/s00382-003-0317-5.

Gao, Y., Drange, H. and Bentsen, M. 2003. Effects of diapycnal and isopycnal mixing on the ventilation of CFCs in the North Atlantic in an isopycnic coordinate OGCM. *Tellus* **55B**, 837–854.

Gao, Y., Drange, H., Bentsen, M. and Johannessen, O. M. 2004. Simulating transport of non-Chernobyl ^{137}Cs and ^{90}Sr in the North Atlantic-Arctic region. *J. Environ. Radioactivity* **71**, 1–16, doi: 10.1016/S0265-931X(03)00108-5.

Gargett, A. 1984. Vertical eddy diffusivity in the ocean interior. *J. Mar. Res.* **42**, 359–393.

Gaspar, P., 1988. Modeling the seasonal cycle of the upper ocean. *J. Phys. Oceanogr.* **18**, 161–180.

Harder, M., 1996. *Dynamik, Rauhigkeit und Alter des Meereises in der Arktis*. PhD thesis, Alfred-Wegner-Institut für Polar- und Meeresforschung, Bremerhaven, Germany.

Hatun, H., Sando, A., Drange, H. and Bentsen, M. 2005. Seasonal to decadal temperature variations in the Faroe-Shetland inflow waters. In: *Climate of the Nordic Seas*, American Geophysical Union Geophysical Monograph. American Geophysical Union, Washington, DC, pp. 239–250.

Hibler, W. 1979. A dynamic thermodynamic sea ice model. *J. Phys. Oceanogr.* **9**, 815–846.

Hurrell, W. 1995. Decadal trends in the North Atlantic oscillation: regional temperatures and precipitation. *Science* **269**, 676–679.

Kalnay, E., Kanamitsu, M., Kistler, R., Collins, W., Deaven, D. and co-authors 1996. The NCEP/NCAR 40-year reanalysis project. *Bull. Am. Meteorol. Soc.* **77**, 437–471.

Karcher, M. J., Gerland, S., Harms, I. H., Iosjpe, M., Heldal, H. E. and co-authors 2004. The dispersion of ^{99}Tc in the Nordic Seas and the Arctic Ocean: a comparison of model results and observations. *J. Environ. Radioactivity* **74**, 185–198.

Kershaw, P. and Baxter, A. 1995. The transfer of reprocessing wastes from north-west Europe to the Arctic. *Deep Sea Res.* **42**, 1413–1448.

Levitus, S. and Boyer, T. P. 1994. *World Ocean Atlas 1994 Volume 4: Temperature*. NOAA Atlas NESDIS 4. NOAA, Washington, DC.

Levitus, S., Burgett, R. and Boyer, T. P. 1994. *World Ocean Atlas 1994 Volume 3: Salinity*. NOAA Atlas NESDIS 3. NOAA, Washington, DC.

Livingston, H., Kupferman, S., Bowen, V. and Moore, R. 1984. Vertical profile of artificial radionuclide concentrations in the central Arctic Ocean. *Geochim. Cosmochim. Acta* **48**, 2195–2203.

McDougall, T. and Dewar, W. 1998. Vertical mixing, cabbeling and thermobaricity in layered models. *J. Phys. Oceanogr.* **28**, 1458–1480.

Nies, H., Harms, H., Karcher, M., Dethleff, D., Bahe, C. and co-authors 1998. Anthropogenic radioactivity in the Nordic Seas and the Arctic Ocean—results of a joint project. *Deut. Hydrograph. Z.* **50**, 313–343.

Nilsen, J. E. Ø., Gao, Y., Drange, H., Furevik, T. and Bentsen, M. 2003. Simulated North Atlantic–Nordic Seas water mass exchanges in an isopycnic coordinate OGCM. *Geophys. Res. Lett.* **30**, 1536, doi:10.1029/2002GL016597.

Orvik, K. and Skagseth, Ø. 2003. The impact of the wind stress curl in the North Atlantic on the Atlantic inflow to the Norwegian Sea toward the Arctic. *Geophys. Res. Lett.* **30**, 1884, doi:10.1029/2003GL017932.

Østerhus, S., Turrell, W R., Jonsson, S. and Hansen, B. 2005. Measured volume, heat, and salt fluxes from the Atlantic to the Arctic Mediterranean. *Geophys. Res. Lett.*, **32**, L07 603, doi:10.1029/2004G1022188.

Poole, A., Denoon, D. and Woodhead, D. 1997. The distribution and inventory of ^{137}Cs in subtidal sediments of the Irish Sea. *Radioprot. -Coll.* **32**, 263–270.

Toggweiler, J., Dixon, K. and Bryan, K. 1989a. Simulations of radiocarbon in a coarse-resolution world ocean model, 1, Steady state prebomb distributions. *J. Geophys. Res.* **94**, 8217–8242.

Toggweiler, J., Dixon, K. and Bryan, K. 1989b. Simulations of radiocarbon in a coarse-resolution world ocean model, 2, Distributions of bomb-produced carbon 14. *J. Geophys. Res.* **94**, 8243–8264.

Willey, B. A., Fine, R. A., Sonnerup, R. E., Bullister, J. L. and Smethie, W. M. 2004. Global oceanic chlorofluorocarbon inventory. *Geophys. Res. Lett.* **31**, doi:10.1029/2003GL018816.

Woodhead, D. and Pentreath, R. 1992. The dispersal of radionuclides in the sea. In: *The Treatment and Handling of Wastes* (eds A. Bradshaw, R. Southwood and F. Warner), Chapman and Hall, London, pp. 131–152.